PFC/JA-83-14

Effects of Plasma Elongation on Magnetics of Continuous-Coil Tokamak Reactors

E. Bobrov
Francis Bitter National Magnet Laboratory

and

L. Bromberg
Plasma Fusion Center

Massachusetts Institute of Technology
Cambridge, MA 02139

April 1983

EFFECTS OF PLASMA ELONGATION ON MAGNETICS OF CONTINUOUS-COIL TOKAMAK REACTORS

E. Bobrov
Francis Bitter National Magnet Laboratory
Massachusetts Institute of Technology
and
L. Bromberg
Plasma Fusion Center
Massachusetts Institute of Technology
Cambridge, MA 02139

ABSTRACT

The paper presents the results of a scoping study of the effects upon machine parameters of varying plasma elongation, aspect ratio and other geometric variables. The toroidal magnets under consideration were designed to have the same ignition margin and constant maximum equivalent membrane stress in the throat of the machine.

1 INTRODUCTION

It is widely believed that plasma shaping allows larger plasma pressures in tokamak devices than possible in circular plasmas. This effect has been used in reactor studies[1]. The effect of elongation on magnetics has been widely studied as it affects the poloidal field system, which provides the elongation. Problem areas lie in the well known vertical instability which may require some form of feedback stabilization; in the larger requirements of the vertical field system, resulting in increased stored energy and in the need of locating poloidal field coils in the bore of the toroidal field magnet.

The effects of elongation on the toroidal field magnet have not been studied as extensively. This is because of the use in these reactor studies of D-shape coils, which allow for relatively large elongations without resulting in larger toroidal field coils (in these coils, the height of the magnet is determined by toroidal field

ripple requirements or by maintenance schemes, which in turn are determined by the location of the outer leg of the magnet).

For continuous coil magnets, the tradeoffs are not as clear. The continuous coils are positioned so close to each other that the toroidal field ripple is almost negligible and both the inplane and out-of-plane loads, as well as the structural reaction to them can be considered as entirely rotationally symmetric.

In a continuous coil magnet, the TF coil can be placed as close as possible to the plasma (allowing spacing for first wall, blankets and shields). The plasma elongation has a direct effect on the shape of the magnet. As a consequence, the stresses in the throat of the magnet and the shearing stresses resulting from the torque action from out-of-plane forces are affected by the plasma elongation.

In this paper, a parametric study for continuous magnets with varying elongation is performed. The parametric study is relevant to the LITE-type of devices, presented elsewhere in this conference[2]. In order to conduct the study, the ignition margins and the stresses in the throat of the magnet are kept constant.

In the next section, a model of the magnet is described. A model for the plasma is analyzed in section 3. The results are presented in section 4.

2 MODEL OF THE MAGNET

The toroidal field coil is of Bitter design. The magnet is an array of 384 copper Bitter plates slit in the median plane at the outer boundary current path. The form of a Bitter plate coil is shown in Figure 1.

The basic unit of the magnet is a turn consisting of a copper plate, a steel reinforcing wedge, two insulating sheets and an interconnector. Keys are inserted between plates and the steel reinforecement to provide shearing capacity for the purpose of transmitting the vertical forces between upper and lower magnet halves between ports and adjacent to ports where the copper plates are split. The keys also transmit shears induced by out-of-plane loading on the magnet. Calculations indicate that virtually all torque is resisted by the outer leg.

The steel reinforcement performs several functions. It transmits the vertical force in the outer limbs of the copper plates. It supports the keys that resist torsional and interplate stress. It provides support for the blanket and other components within the TF coil. In the center of each half module it furnishes

extra turn spacing to improve the homogeneity of the toroidal field. The steel is flush with the copper at the outer edges but extends beyond it toward the plasma to support the blanket and first wall assembly.

Each turn has two sheets of insulation. The keys are fully insulated from the steel reinforcement which is everywhere at ground potential. The insulation extends beyond the plates to ensure that shorts do not occur at exposed edges. The insulation is polyimide-glass reinforcement sheets.

The structural behavior of the TF magnet is analyzed here on the basis of the orthotropic toroidal shell model proposed in 1981 by Bobrov and Schultz [3]. The model treats the toroidal field coil assembly, which is subjected to both in-plane and out-of-plane loads, as a thick continuous orthotropic shell. The thicknesses and elastic moduli of the shell vary with the major radius. The model is capable of handling the presence of cooling passages, various ports and keys between the laminations of the Bitter plates.

Initial structural studies indicated that if the outer contour of a rectangular Bitter plate is modified by cropping the corners so that the outer contour is more consistent with the contour of the magnet bore, the stress situation in the throat of the magnet would improve. In addition, by cutting off the corners of a rectangular plate, more room is created for positioning the ohmic heating coils and the equilibrium field coils, as shown in Figure 1, and the weight is reduced.

The vertical radial cross-section of the toroidal magnet and the thick toroidal shell model outline are shown in Figure 1. The inner and outer surfaces of the shell are generated by rotation of two eccentric ellipses (A and B) about the toroidal axis $R = 0$. The computer code generates all the geometric parameters of the midsurface of the orthotropic toroidal shell of varying thickness. These parameters include the major toroidal radii, principal radii of curvature, thickness and the effective elastic moduli.

3 MODEL OF THE PLASMA

In this section the plasma model is described.

It is assumed that the plasma average β (the ratio between the plasma pressure and the magnetic field pressure) scales as

$$\beta = .105\frac{\kappa}{A}$$

where $\kappa = b/a$ is the elongation and A is the aspect ratio. It is assumed that the plasma safety factor q is 2.5. For an aspect ratio of $A \sim 3.3$ and $\kappa = 1.6$ (the illustrative design of LITE^2), $\beta = 0.05$.

It is assumed that the energy confinement for the electrons is given by the empirical scaling law[4]

$$\tau_{E_e} = 3.8 \times 10^{-21} n a^2 \kappa$$

where n is the average plasma density in m^{-3}, a is the minor radius in m and τ_{E_e} is in seconds.

The margin of ignition is then

$$MI = \frac{(n\tau_E)_{empirical}}{(n\tau_E)_{ignition}} \sim (\beta_T a B^2)^2 \kappa$$

at fixed temperature. From transport calculations it has been determined that the value of $(\beta_T a B^2)^2 \kappa$ at ignition is $\left((\beta_T a B^2)^2 \kappa\right)_{ignition} = 1.3\ \mathrm{m^2 T^4}$ for parabolic density and temperature profiles and in the absence of impurities. Therefore,

$$MI = \frac{(\beta_T a B^2)^2 \kappa}{((\beta_T a B^2)^2 \kappa)_{ignition}} = \frac{(\beta_T a B^2)^2 \kappa}{1.3}$$

where a is in m and B is in T. MI is a measure of how close the plasma is to ignition according to the empirical scaling law or, if $MI > 1$, of the margin of safety to achieve ignition.

In the results reported in this paper, MI has been held constant.

The requirements of the vertical field are calculated using the results from reference 5. Fast and accurate description of the required coil currents are obtained using the results presented therein.

The requirements of the ohmic heating system are calculated using the model described in reference 5.

4 RESULTS

The results from the parametric scan are presented in this section.

The following stress parameters are used to evaluate the structural effectiveness of the magnet: the membrane equivalent von Mises stresses in the throat of the coil, σ_{mem}, the peak membrane-plus-bending stresses in the magnet $\sigma_{mem+bend}$ (which occur in the throat of the magnet on the inner fiber of the plate), the maximum tangential shear stress between plates reacting the out of plane loads τ, the integral of the absolute value of the shear Σ_{shear}, and the integrated reactive torque Θ. It should be noted that the peak shear stress in all cases considered takes place in the vicinity of the port.

Table 1 shows the assumptions for the parametric study. The equivalent von Mises stresses in the throat of the magnet are kept constant to 230 MPa. At these levels, the magnet should last for $\gtrsim$ 1000 pulses when operated at liquid nitrogen temperature. The tokamak would operate at lower stresses ($\sigma_{mem} \sim$ 140 MPa) at room temperature. The operational scenario is discussed in reference 2. The size of the OH transformer is determined by assuming a burn pulse of 100 s and peak stresses in the OH transformer of 140 MPa. The central electron temperature during burn is 15 keV.

Table 2 shows the results of the parametric study when the aspect ratio is varied. The plasma elongation is assumed to be 1.6 in this table. B is the magnetic field on the plasma axis, I_p is the plasma current, P_{wall} is the average neutron loading at the plasma surface, P_f is the fusion power, E_{TF}, P_{TF} and W_{TF} are the stored energy, the resistive power and the weight of the toroidal field system, E_{OH} and P_{OH} are the stored energy and peak resistive power of the OH transformer at the beginning of the pulse, E_{EF}, P_{EF}, W_{EF} and MA_{EF} are the stored energy, resistive power, weight and Ampere turns of the vertical field system.

As the aspect ratio is decreased, the wall loading decreases. The fusion power has a minimum of $P_f \sim$ 1.3 GW for $A \sim 3 - 4$. The resistive power and the stored energy in the toroidal field coil have a broad minimum about $A \sim 3$. The poloidal field system (OH and EF systems) have a broad minimum for $A \sim 3.5 - 4.5$. The shear stresses, the integrated shear and the bending in the throat of the magnet decrease monotonically with decreasing aspect ratio.

Figures 2 and 3 show the the stress variation with the poloidal angle, for the

case in Table 2 with $A = 3.3$ (the illustrative design of LITE presented elsewhere at this meeting[2]). Figure 2 presents the inplane stresses σ_{mem} and $\sigma_{mem+bend}$, at the inner fiber of the plate. Shown in Figure 3 is the shear stress τ. The angle θ is measured from the centroid of the magnet R_m, and is 0 at the throat midplane. There is a region in the throat with large membrane stresses, which decrease rapidly away for $\theta \sim \pi/3$. The shear stresses due to the out-of-plane loads are small in the region of the coil away from the ports. In the region of the ports, the shear stresses are relatively flat and peak to about 10 MPa.

In Table 3, the plasma elongation is varied. The aspect ratio is kept constant at about $A = 3.3$, and β is assumed to vary linearly with κ. In general, the toroidal field system becomes simpler at the expense of the poloidal field system getting more complex. Note that the total resistive power of the toroidal and poloidal field systems is approximately constant as the elongation is varied. The plasma major radius decreases with increasing elongation. Increasing the plasma elongation has also the effect of decreasing the bending in the throat region and the shear stresses in the vicinity of the ports. Therefore, if the goal is to keep the margin of ignition fixed, increasing the elongation has advantages, due to the increased τ_e and β with increasing elongation. However, the advantages of operating at large values of elongation are partially balanced by increased complexity in the poloidal field system (which would require complex control systems to provide vertical stability) and increased extrapolation from present experimental results.

Tables 4 — 6 show the variations in the illustrative design of LITE as the stresses in the throat of the magnet (Table 4), the height of the magnet (Table 5) and the build of the outer leg (Table 6) are varied. Decreasing the stresses σ_{mem} by $\sim 10\%$ results in a $\sim 5\%$ increase in major radius and resistive power and $\sim 15\%$ increase in stored energy. The vertical field system is only slightly affected.

Increasing the height of the magnet is a way of controlling the bending in the throat of the magnet. The membrane stresses do not change. The minor decrease in bending in the throat is balanced by increases in the requirements for the poloidal field system.

Finally, Table 6 shows the variations in the illustrative design as the build of the outer leg t_o in decreased. The resistive power and the shear stresses τ increase. The latter increases not as strongly as inversely porportional to the build of the outer leg due to a decreased overturning moment, resulting from an

EF coil location that is closer to the plasma.

CONCLUSIONS

A scoping study has been performed of continuous-coil tokamaks. The study shows that there is a wide range of design space where the major subsystems remain approximately constant. Further study is necessry to find the optimum design.

ACKNOWLEDGMENTS

This work was funded by the U.S. Department of Energy. The Francis Bitter National Magnet Laboratory is supported by the National Science Foundation.

REFERENCES

1 BAKER, C.C., "Tokamak reactor studies", Proceedings of the IEEE, **69** (1981) 917.

2 BROMBERG, L., COHN, D.R., WILLIAMS, J.E.C., JASSBY, D.R. and OKABAYASHI, M., "A Long Pulse Ignited Test Experiment", presented elsewhere at this conference, paper P-1.

3 BOBROV, E. and SHULTZ, J., "Analysis of toroidal magnet systems on the basis of the Reissner shell theory", MIT Plasma Fusion Center Report PFC/JA-82-10

4. COHN, D.R., PARKER, R.R. and JASSBY, D.L., "Characteristics of high density tokamak ignition reactors", Nucl. Fusion **16** (1976) 31; JASSBY, D.L., COHN, D.R. and PARKER, R.R., "Reply to comments on characteristics of high density tokamak ignition reactors", Nucl. Fusion **16** (1976) 1045.

5 BOBROV, E., BROMBERG, L., COHN, D.R., DIATCHENKO, N., LECLAIRE, R.J., MEYER, J.E. and WILLIAMS, J.E.C., "High Field Tokamaks with DD-DT Operation and Reduced Tritium Breeding Requirements", MIT Plasma Fusion Center Report PFC-RR-83-5 (Nov 1982)

Table 1
Constraints for Scoping Study

MI	8.5
σ_{mem} (MPa)	230
$c_\beta = \beta A/\kappa$	0.105
q	2.5
T_{eo} (keV)	15
burn pulse lengths (s)	100
σ_{OH}(Double Swung) (MPa)	140
Δ_i(m)	0.25
Δ_t(m)	0.25
Δ_o(m)	0.55
port size (height $\times$ width) (m^2)	0.8×0.5
Number of ports	16

Table 2
Parametric Scan for $\sigma_{TF} = 230$ MPa and
$MI = 8.5$ as Function of Aspect Ratio

A	2.35	2.73	3.1	3.37	4.23	7.14
R (m)	3.52	3.0	2.79	2.7	2.75	4.14
a (m)	1.5	1.1	0.9	0.8	0.65	0.58
B (T)	4.94	6.22	7.33	8.1	10.0	13.8
I_p (MA)	14.7	11.5	9.63	8.62	6.74	4.67
P_{wall} (MW/m^2)	5.06	6.91	8.44	9.44	11.3	12.9
P_f (GW)	1.67	1.42	1.32	1.27	1.26	1.93
E_{TF} (GJ)	4.42	3.77	3.73	3.80	4.81	15.2
P_{TF} (MW)	299	288	295	308	378	830
W_{TF} (Gg)	4.1	2.78	2.25	2.03	1.90	3.31
E_{OH} (GJ)	4.06	2.33	1.75	1.49	1.22	1.7
P_{OH} (MW)	185	149	136	128	117	130.
E_{EF} (GJ)	1.43	1.02	0.869	0.826	0.874	2.7
P_{EF} (MW)	211	166	147	140	142	276
W_{EF} (Gg)	0.419	0.331	0.293	0.28	0.283	0.534
MA_{EF} (MA turn)	29.5	25.4	22.9	22.1	21.6	29.4
$\sigma_{mem+bend}$ (MPa)	261	271	278	291	309	332
τ (MPa)	2.4	5.2	7.83	10.8	19.6	39.4
Σ_{shear} (MN)	11.2	11.9	13.0	13.8	17.3	38.9
Θ (MN m)	6.7	12.4	17.0	20.0	30.6	103.

Table 3
Parametric Variation vs. Elongation
$MI = 8.5$, $\sigma_{TF} = 230$ MPa

κ	1.2	1.4	1.6	1.9
R (m)	3.21	2.89	2.7	2.46
a (m)	0.965	0.861	0.8	0.745
B (T)	9.07	8.6	8.1	7.28
I_p (MA)	8.5	8.5	8.62	9.0
P_{wall} (MW/m^2)	9.01	9.36	9.44	9.14
P_f (GW)	1.51	1.36	1.27	1.14
E_{TF} (GJ)	6.4	4.75	3.80	2.80
P_{TF} (MW)	397	344	308	267
W_{TF} (Gg)	2.79	2.29	2.03	1.78
E_{OH} (GJ)	1.84	1.59	1.49	1.35
P_{OH} (MW)	138	129	128	127
E_{EF} (GJ)	0.373	0.577	0.826	1.23
P_{EF} (MW)	78	112	140	178
W_{EF} (Gg)	0.169	0.228	0.28	0.351
MA_{EF} (MA turn)	8.56	15.9	22.1	31.3
$\sigma_{mem+bend}$ (MPa)	335	311	291	274
τ (MPa)	16.9	11.2	10.8	10.9
Σ_{shear} (MN)	13.3	13.5	13.8	13.6
Θ (MN m)	30.9	24.6	20.0	14.0

Table 4
Parametric Variation vs. σ_{mem}
for $MI = 8.5$

σ_{mem} (MPa)	202.	232.
R (m)	2.89	2.7
a (m)	0.8	0.8
A	3.61	3.37
B (T)	8.39	8.1
I_p (MA)	8.28	8.62
P_{wall} (MW/m^2)	9.48	9.44
P_f (GW)	1.37	1.27
E_{TF} (GJ)	4.48	3.80
P_{TF} (MW)	326.	308.
W_{TF} (Gg)	2.21	2.03
E_{OH} (GJ)	1.52	1.49
P_{OH} (MW)	119.	128.
E_{EF} (GJ)	0.849	0.826
P_{EF} (MW)	143	140
W_{EF} (Gg)	0.286	0.28
MA_{EF} (MA turn)	21.1	22.1
$\sigma_{mem+bend}$ (MPa)	262	291
τ (MPa)	12.0	10.8
Σ_{shear} (MN)	14.5	13.8
Θ (MN m)	22.6	20.0

Table 5
Parametric Variation vs. height of magnet for $MI = 8.5$

h (m)	4.76	4.50
E_{TF} (GJ)	3.92	3.80
P_{TF} (MW)	293	308
W_{TF} (Gg)	2.19	2.03
E_{OH} (GJ)	1.58	1.5
P_{OH} (MW)	136	129
E_{EF} (GJ)	0.91	0.826
P_{EF} (MW)	149	140
W_{EF} (Gg)	0.30	0.28
MA_{EF} (MA turn)	23.7	22.1
σ_{mem} (MPa)	232	231
$\sigma_{mem+bend}$ (MPa)	281	291
τ (MPa)	10.9	10.8
Σ_{shear} (MN)	14.0	13.8
Θ (MN m)	20.0	20.0

Table 6
Parametric Variation vs. t_o
for $MI = 8.5$

t_o (m)	1.5	1.0
E_{TF} (GJ)	3.80	3.64
P_{TF} (MW)	308	328
W_{TF} (Gg)	2.03	1.63
E_{EF} (GJ)	0.826	0.734
P_{EF} (MW)	140	131
W_{EF} (Gg)	0.28	0.26
MA_{EF} (MA turn)	22.1	21.6
σ_{mem} (MPa)	231	232
$\sigma_{mem+bend}$ (MPa)	291	281
τ (MPa)	10.8	12.9
Σ_{shear} (MN)	13.8	11.7
Θ (MN m)	20.0	13.0

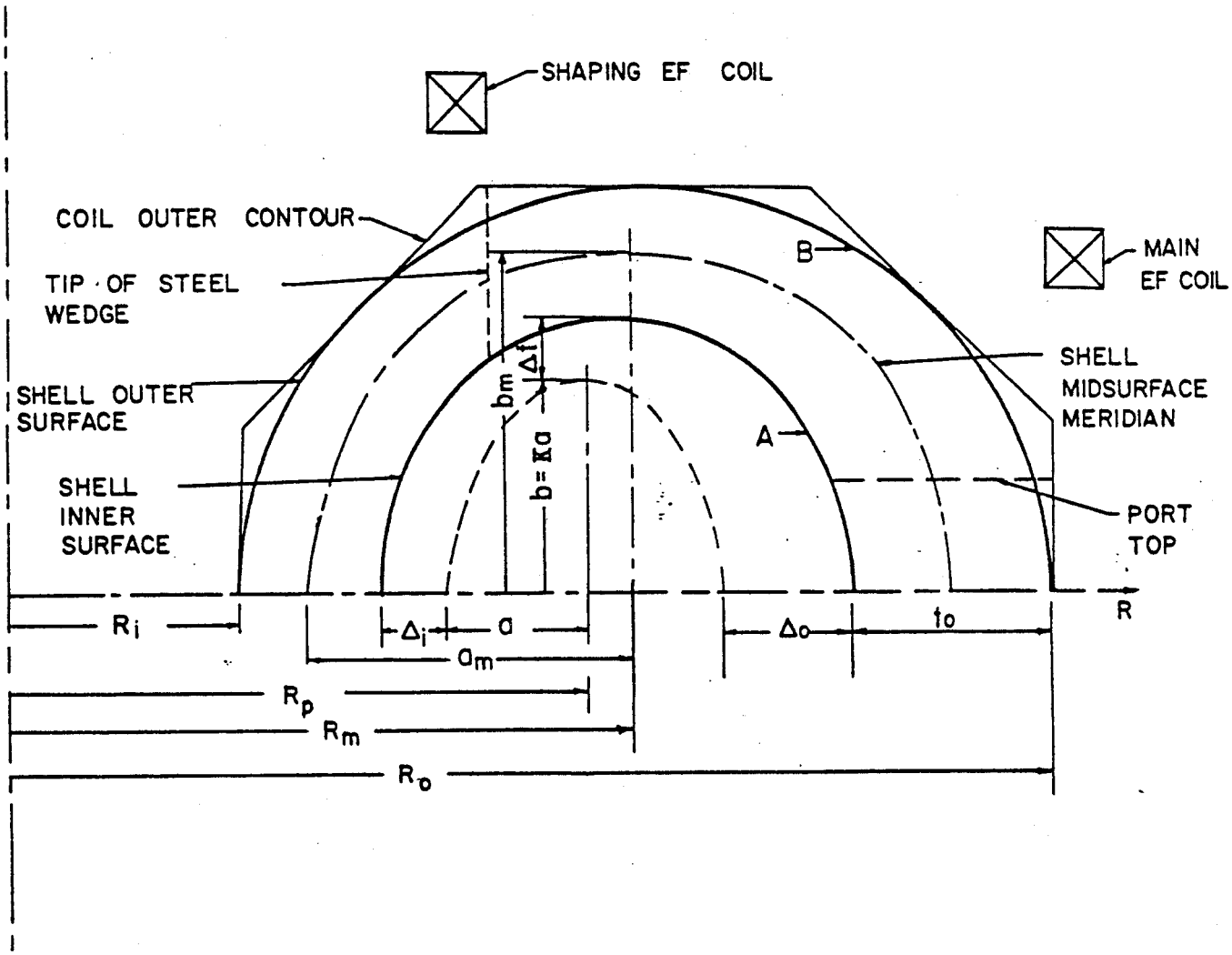

Figure 1 Contours of Bitter plate coil and shell model

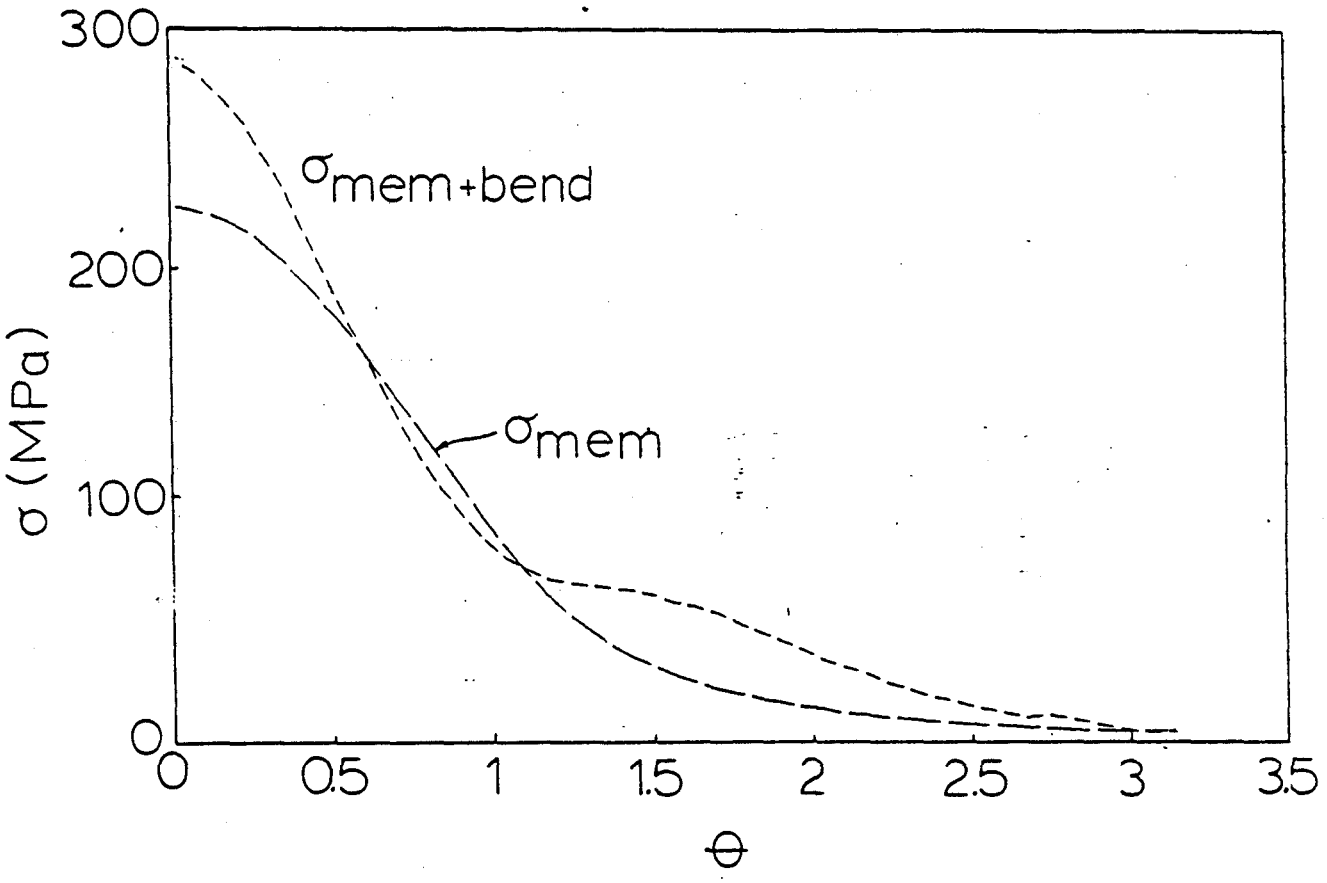

Figure 2 Variation of poloidal stresses in the coil due to inplane loads.

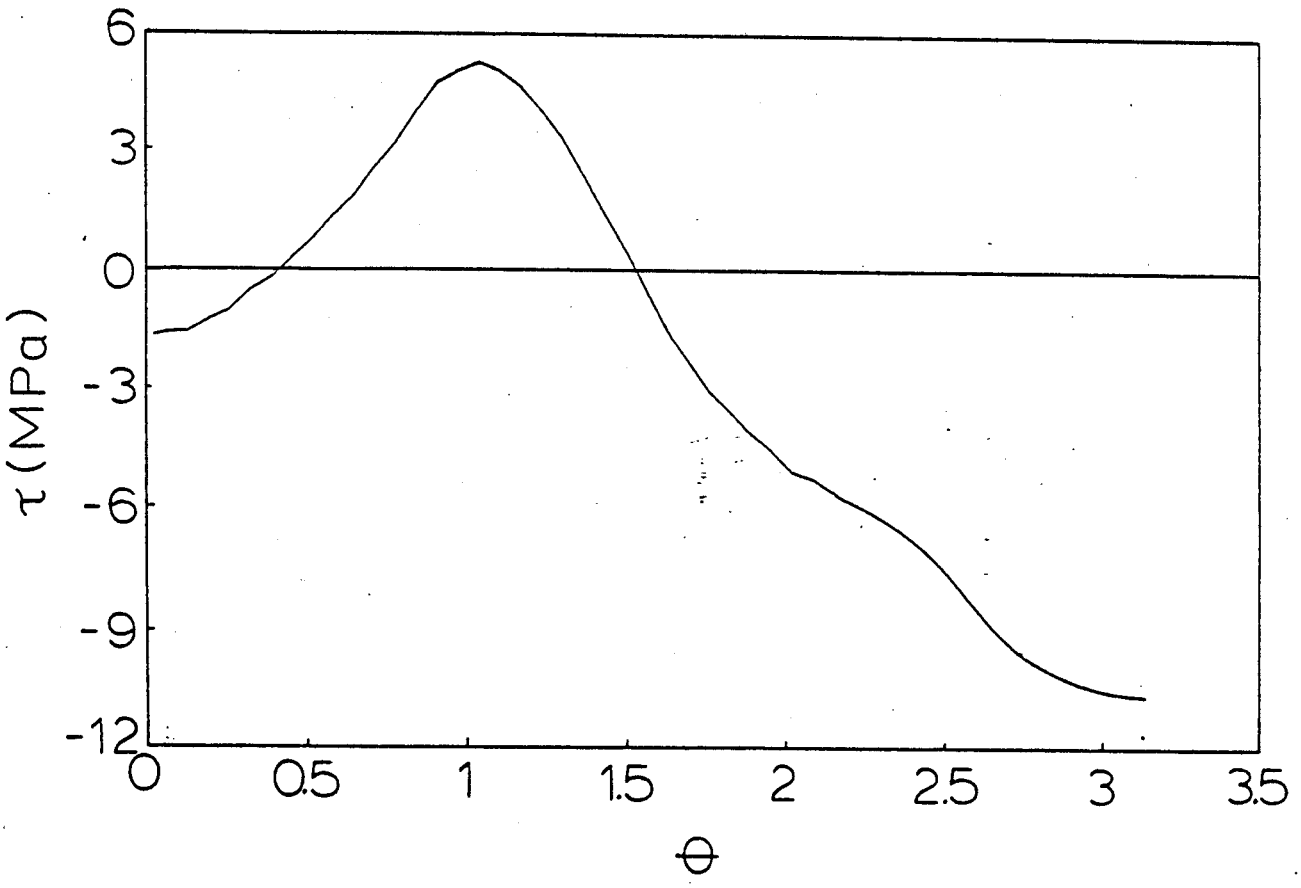

Figure 3 Variation of shear stresses due to out of plane loads